Acoustic Interrogation and Imaging of Complex Sub-surface Seabed Properties

Jacques Y. Guigne, Ryan Laidley, Maria Kotsi, Stephanie Abbott, Cevdet A. Kilic, & Michael Manning

Kraken Robotics, Mount Pearl NL, Canada

Dillon Hoffmann & Kevin Kennelley

Couvillion Group, Louisiana, USA

ABSTRACT: *The Acoustic Corer™ applies collocated transmitters, low-frequency chirps, high-frequency chirps and parametric arrays, which span frequencies from 1.5kHz–5kHz through a stationary landed survey platform. The acoustics are directed at interrogating the sub-seabed to deliver a wide 14m diameter volumetric "acoustic core" down to 60m below seabed. The presented innovation involves a large fusion of multi-cores migrated into a single unified data volume. Rather than mosaicking the individual acoustic cores, the pre-processed data sets are merged and uniformly migrated. This results in enhanced resolution and coherency to provide accurate identification and representation of potential geohazards and stratigraphy. In this study, 63 Acoustic Corer™ (AC) surveys were conducted in the Gulf of Mexico. The detailed results highlighted chaotic mud slide clay blocks within the upper sub-seabed, a densely consolidated basement layer and 18 conductor pipes, not previously identified.*

1 **Introduction**

Three-dimensional (3-D) investigations of the shallow sub-seabed for identifying and characterising geohazards and stratigraphy require specular and non-specular returns with spatial accuracies exceeding those of current conventional seismic surveys (i.e., towed streamer-based methods). Advanced acoustic accuracies enable improved correlations between acoustic and geotechnical properties of near-surface soils. To effectively image geohazards (e.g., boulders, pipes, etc.) and stratigraphic characteristics (e.g., small-scale sand/shale lenses) requires retention of the entire signal energy distributions, principally the diffuse diffracted signals and the dominating reflective energy and location calibrations. This is accomplished by sub-seabed interrogation through a stationary transmitter and receiver spatial centimeter-spaced network with horizontal dimensions greater than 5m (16ft).

The study area chosen to develop the innovation herein was within the Gulf of Mexico. Kraken Robotics (formerly PanGeo Subsea, a subsidiary of Kraken Robotics) carried out a sub-bottom/below mudline (BML) survey, where 63 Acoustic Corer™ (AC) scans were completed to determine the extent, expanse, orientation and characteristics of conductor pipes. The survey area was 205m (673ft) x 60m (197ft) (Figure 1). The acoustic core results provided a 14m (46ft) diameter volumetric image of the sub-bottom down to a penetration depth of approximately 60m (200ft).

2 **Acoustic Corer™ (AC)**

The approach called "Acoustic Sub-seabed Interrogation" (ASI) was first introduced by Guigné in 1986 at the University of Bath (Guigné, 1986). This technique was designed to acquire the backscattering response of discrete targets within the sub-seabed using a dense data acquisition grid (Clark & Guigné, 1988; Guigné & Chin, 1989).

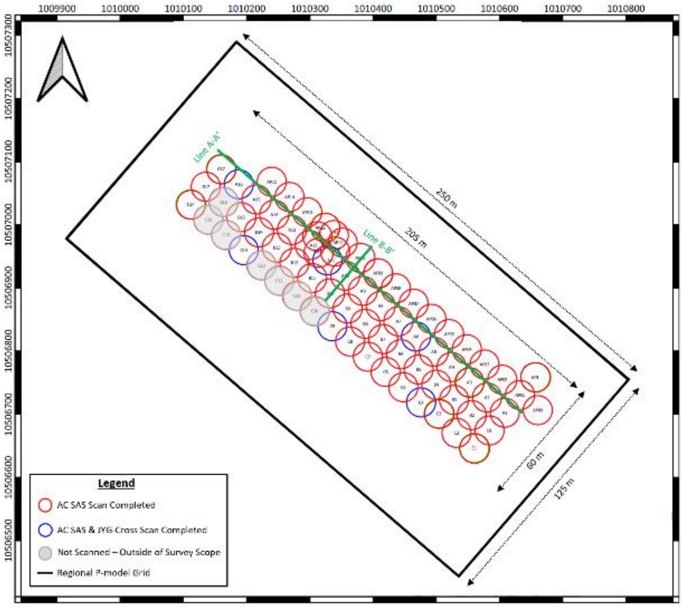

Figure 1 - Sixty-three (63) acoustic core survey area layout

The first ASI design was developed and tested from 1990 to 1996 (Inkpen et al., 1991). The experimental model involved a platform that supported 16 planar sparker transmitters in an octagonal polyethylene framework held by an aluminum outer structure. A 12m-long (39ft) rotating boom at the apex of the instrument provided support to 12 equally spaced calibrated hydrophones. The 12 receivers were rotated during data collection and aligned with four transmitters to form a transmitting-receiving row called a “beam”, delivering four linear “beams” of data. The resulting data was processed and rendered into a 3-D volumetric image having a minimum 10m diameter (33ft) with a sub-sea penetration depth of over 10m (33ft). This stationary acoustic acquisition “lens” provided an “Acoustic Core” solution involving a 3-D determination of geophysical parameters of the subsurface, while maintaining signal coherence between repeated echoes.

Since 2006, it has been further developed and trademarked as the “Acoustic Corer™ (AC)” (Guigné et al., 2010; Guigné et al., 2012; Guigné, 2014; Guigné & Blondel, 2017). The AC comprises sonar hardware and data collection, advanced data processing and interpretation software. The approach is designed to acquire a full wavefield response of the first 60m (200ft) of complex sub-seabeds.

2.1 *Hardware Description*

The AC consists of two sonar heads attached to each arm of a 12m (39ft) boom held and rotating off a set of tripod legs (Figure 2). This boom turns 180°, creating a 360° acoustic core product 14m (46ft) in diameter down to a depth of 60m (200ft). The sonar heads contain three collocated acoustic sensors: an HF chirp (operating across 4.5–12.5kHz), an LF chirp (operating across 1.5–6.5kHz) and a Parametric source (using a secondary frequency (f_s) of 8kHz) (Table 1 and Figure 3). The Parametric source has a narrower acoustic propagation pattern than the HF chirp which provides more detailed, crisper imagery of the features. Together with the HF chirp, collocated confidence is derived and critical imagery elements are confirmed in target picking.

Figure 2 - Standard Acoustic Corer™ deployment configuration

2.2 *Theoretical Background*

The modelling and imaging of targets are governed by the acoustic wave equation under the assumption of a gradient-density medium. Every target is modelled as discrete, compactly supported perturbations of a global background sound speed function defined in the 3-D Cartesian space R^3. The full wave speed function is decomposed as

$$c(x) = c_o(x) + \Delta c(x)$$

where c_o represents a smooth background model and Δc represents any diffractions or scatterers. The acoustic wave equation in the frequency domain (Helmholtz equation) has the form:

$$\left(\nabla^2 - \omega^2/_{c^2}\right) u(x, x_s, \omega) = \delta(x - x_s)$$

where ω is the angular frequency, u is the full wavefield and δ is the dirac delta function.

Following the Born geometric optics approximations, the scattered wavefield can be expressed in the frequency domain as:

$$u(x, x_s, \omega) = -\omega^2 \int_\Omega u_i^0(\xi, x_s) u_i^0(\xi, x) e^{i\omega(\tau(\xi,x_s)+\tau(\xi,x))} \Delta^2 s(\xi) d\xi$$

Using the generalised back-projection operator from Beylkin (1985) the imaging operator is defined as

$$R^* u_s(x) = \int_{\delta\Omega} u_s(\xi, x_s, \phi(x, x_s, \xi)) w(x, x_s, \xi) d\,\xi$$

This imaging operator is recognised as a weighted diffraction summation (integration) over the aperture of the recorded data. Explicitly, the summation is carried out over the diffraction curve defined by φ and scaled by w.

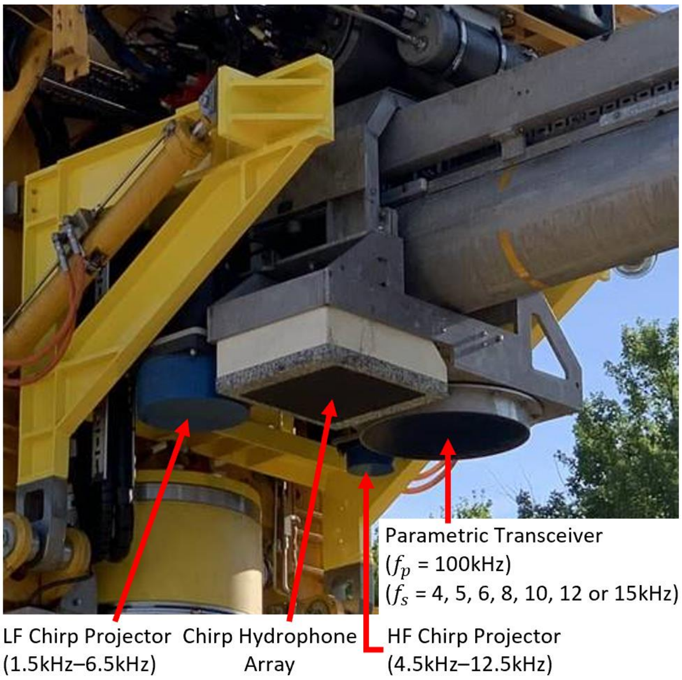

Figure 3 - Three AC sources: HF/LF chirps and a Parametric transceiver (f_p = primary frequency, f_s = secondary frequency)

Table 1 - Acquisition parameters for the three AC sources

Setting	High-Frequency (HF)	Low-Frequency (LF)	Innomar/Parametric
Sampling Rate	50kHz	50kHz	100kHz
Samples Per Trace	5450	5450	7333
Penetration Depth	60m	60m	60m
Pulse Frequency Range	4.5–2.5kHz	1.5–6.5kHz	8kHz (f_s)
Pulse Segment (Chirp) Duration	15ms	15ms	N/A
Pulse Width (Innomar/Parametric)	N/A	N/A	0.07–1ms (User Selectable)
Pulse Taper Type (Waveform)	Rectangular	Rectangular	N/A
Pulse Type	Linear	Linear	Ricker
Match Filter Type	Hann	Hann	N/A
Ambient Noise Recording	ON	ON	ON

3 Survey Area

3.1 *Geotechnical Information of the Survey Area*

The survey area is largely comprised of clay with the top 18–21m (59–69ft) suggestive of mass flow deposits. As a result, this material is highly variable with undrained shear strengths approaching zero near the mudline (i.e., seabed surface), increasing to about 26.3kPa around 23m (75ft) BML. However, harder material could still be encountered at shallower depths depending on whether blocky material exists within the mass transport deposits. Below 23m (75ft), the soil is less variable but under-consolidated with undrained shear strengths ranging from 28.7–33.5kPa between 24–61m (78–200ft) BML. These shear strengths are nearly 3 times lower than those typically encountered in other regions of the Gulf of Mexico.

3.2 *Data Acquisition*

The uppermost seabed (7.3m (24ft) BML) is characterised by soft sediments with low shear strength (<10kPa). These conditions required close stability monitoring during deployment of the AC using a crane. Immediately after landing and transferring the weight of the AC to the seabed, the AC's depth, altitude, pitch and roll were recorded and stability tests were performed. Having determined that the system was stable in static mode, the AC was rotated and acoustic payloads moved out of the booms to their baseline positions while continually monitoring pitch, roll and altitude via the onboard sensors located on the main frame and acoustic payloads.

4 Survey Area

4.1 *JYG-Cross and Regional P-model Generation*

The JYG-Cross (Guigné et al., 2010) is a technique that resembles a high-precision seismic line that folds the data to accentuate sub-seabed stratigraphy, similar to multichannel marine seismology. It collects approximately 5000 data points along two pseudo-orthogonal lines using the LF chirp at an interval spacing of 10cm (4in) (Figure 4). These data sets are used to perform 2-D semblance analysis (Figure 4) to derive soil velocity profiles (V_{rms}) and subsequent velocity models. Velocity models, (p-models), are 3-D volumes that are generated to provide the coordinates and soil velocities of the points that will be imaged.

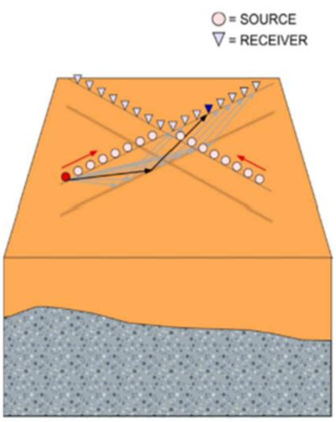

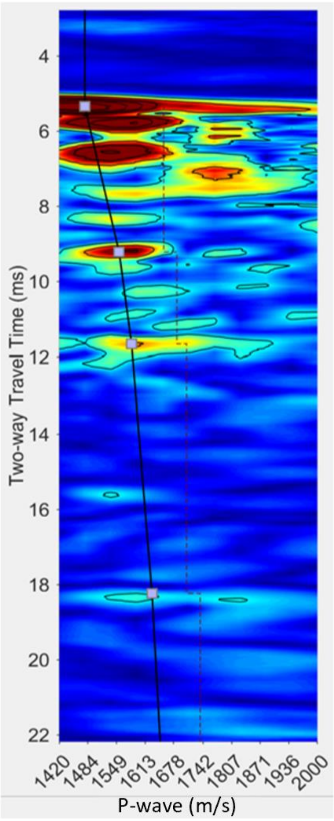

Figure 4 - Left: JYG-cross data acquisition configuration; Right: Semblance analysis (i.e., velocity profiles) for p-model creation

In this study, JYG-Cross data was collected at six scan locations throughout the survey area (Figure 1) and six velocity profiles (V_{rms}) were generated (Figure 4). These V_{rms} profiles were then used in a gridded interpolation to generate a regional velocity model across the entire survey area, with a size of 250m (820ft) by 125m (410ft) (Figure 1). The utilised X-Y-Z grid had an interval spacing of 10cm by 10cm for the X-Y plane and 0.02ms for the Z-interval.

4.2 *Imaging and Horizon Picking*

All 63 AC volumes were processed through standard seismic processing steps using ZoomSpace™ in-house software. The individual pre-processed volumes were merged and migrated into a single cohesive volume which was statically corrected to the same reference datum. This enabled a more unified identification and interpretation of the conductors. The detailed processing flow is shown in Figure 5.

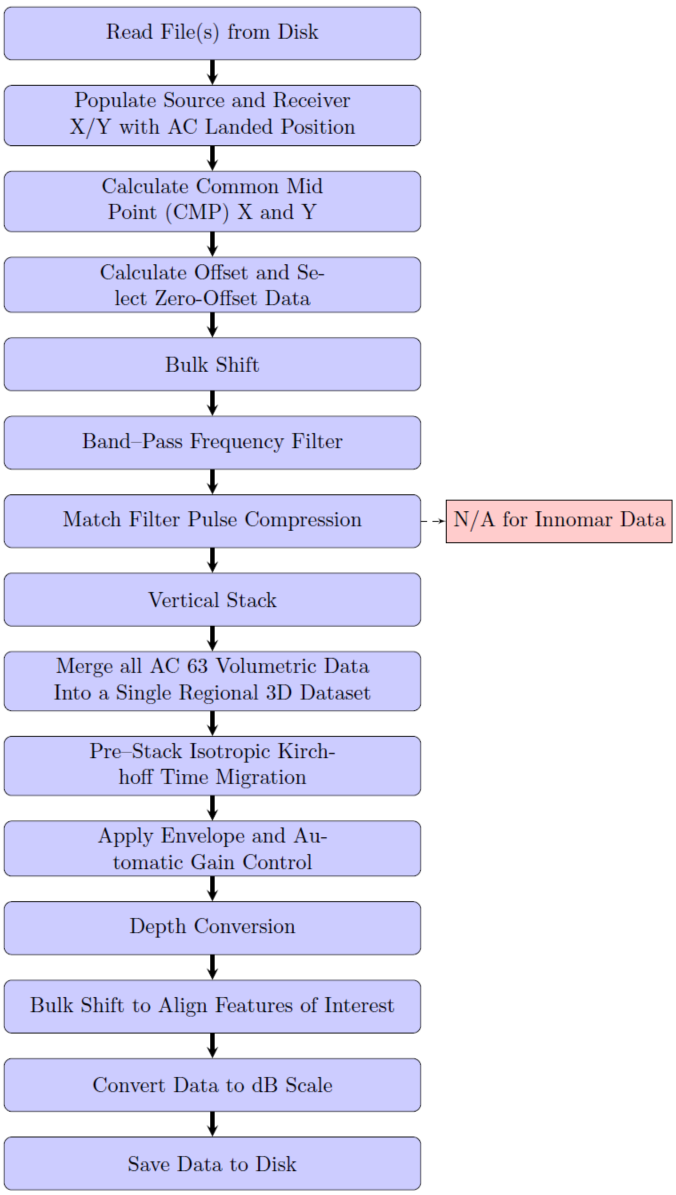

Figure 5 - ZoomSpace™ SAS data processing workflow

For the interpretation and picking of the seabed, conductors and basement horizons, the post-processed migrated volume was analysed using OpendTect software. Initial interpretation began with the seabed, where a grid was generated using the inline/crossline data. Each grid line was tracked along the seabed horizon, appearing as a continuous bright reflector within the data (Figure 6). A similar approach was used to construct a series of grid lines, representing the basement surface. Once completed, a gridding technique was applied using an inverse distance weighted algorithm. The grids were filtered and smoothed using an average-type weighting scheme and the 3-D horizon surfaces were created (Figure 7). The conductors were evaluated in cross-section (inline) view, tracking the bulls-eye response of each feature along the unified dataset (Figure 9). A location point was marked for every visible conductor at each inline interval. This procedure was repeated along the entirety of the migrated volume until the full extent of each individual conductor had been identified. A total of 18 conductors were interpreted, comprising a digitisation of approximately 40–50 location points per conductor. The 18 conductors and the inferred seabed and basement horizons were then imported into EIVA's NaviModel visualisation software for further analysis (Figure 7).

4.3 *Interpretation*

The AC data sets accurately captured not only the specular returning sedimentary signals but more importantly, the non-specular returns of the conductors. They delivered a volumetric image of the conductors' presence characterising their depth, shape, size and form. Notably, a continuous traverse from NW to SE was observed (Figure 8).

In the upper region of the sub-seabed, namely the upper 18m (59ft), the composition is characterised by an unconsolidated chaotic nature, at times blocky, associated with a flow event. In this region, clay-based linear diffractors are present within a weak non-cohesive sediment matrix. Close examination of the reflecting responses of the clay strata supports an assignment of undrained shear strengths associated with a very soft fluid state at the mudline (near 0kPa) to soft denser clay in the strata (12–25kPa).

The conductors appear as a bundle primarily in Lines AP and A (Figure 1) running NW-SE where an apparent, abrupt termination is observed (Figure 6). These conductors are found at depths between 27.7–48.1m (91–158ft), with the greatest concentration appearing between 39.6–47.2m (130–155ft). The shallowest conductor appears at 27.7m (91ft) trending downwards from the toppled jacket (Figure 8). The cross-sectional analysis of the conductor bundle (Figure 9) positively identified 18 individual conductors (Figure 8). By migrating all the cores together, the spatial resolution was improved. This provided additional clarity on the continuity of the conductors and enabled discrimination with a high degree of confidence.

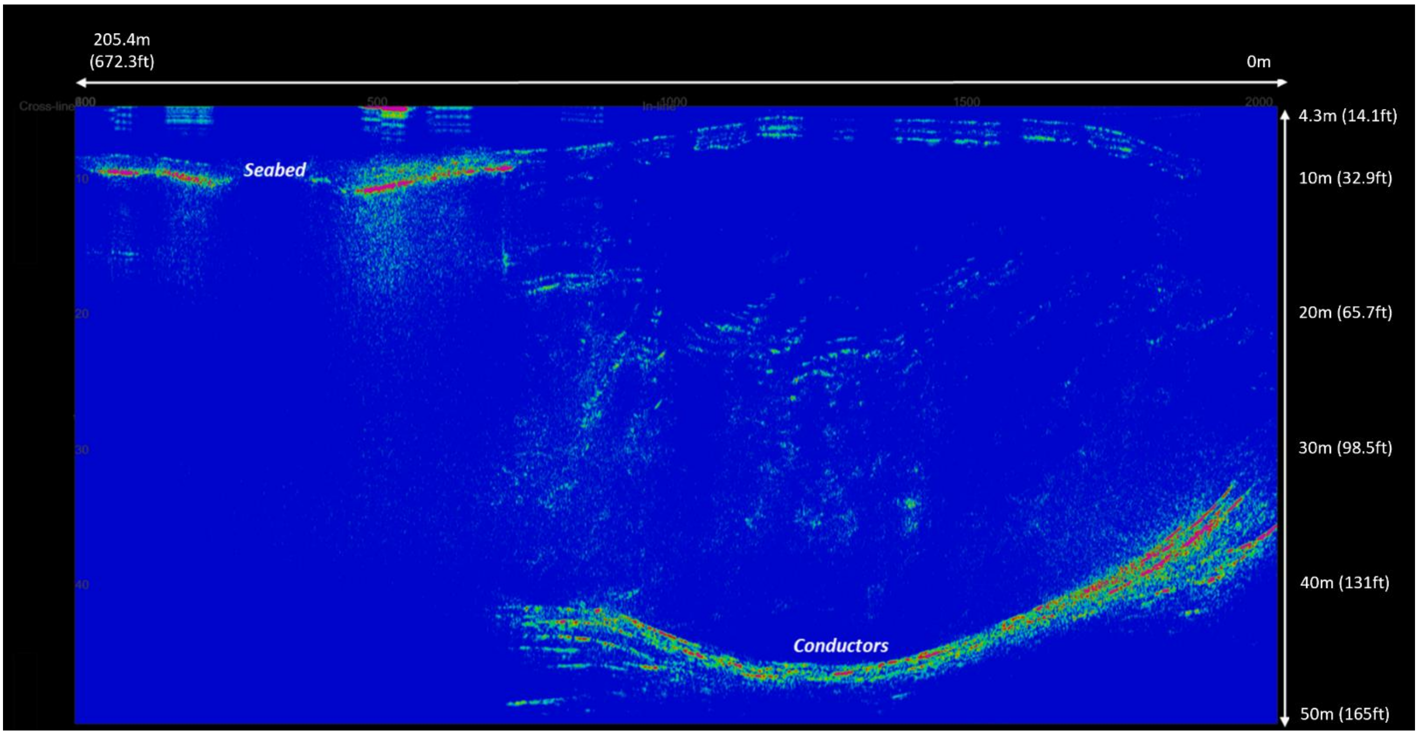

Figure 6 - Crossline 335 (Line A-A’ in Figure 1) of the unified migrated volume highlighting important features of interest

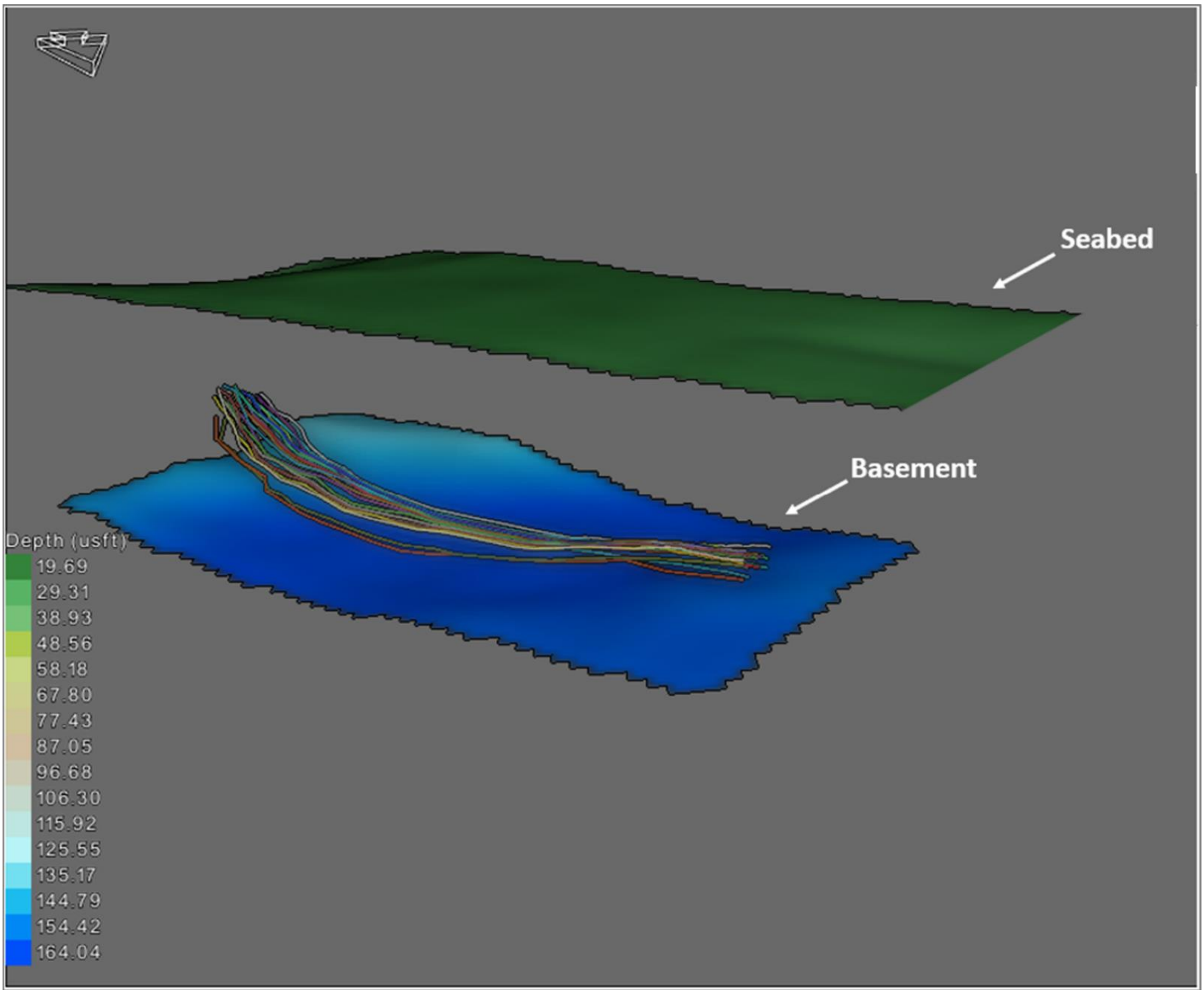

Figure 7 - NaviModel 3-D visualization of the inferred seabed, basement and 18 conductor bundle

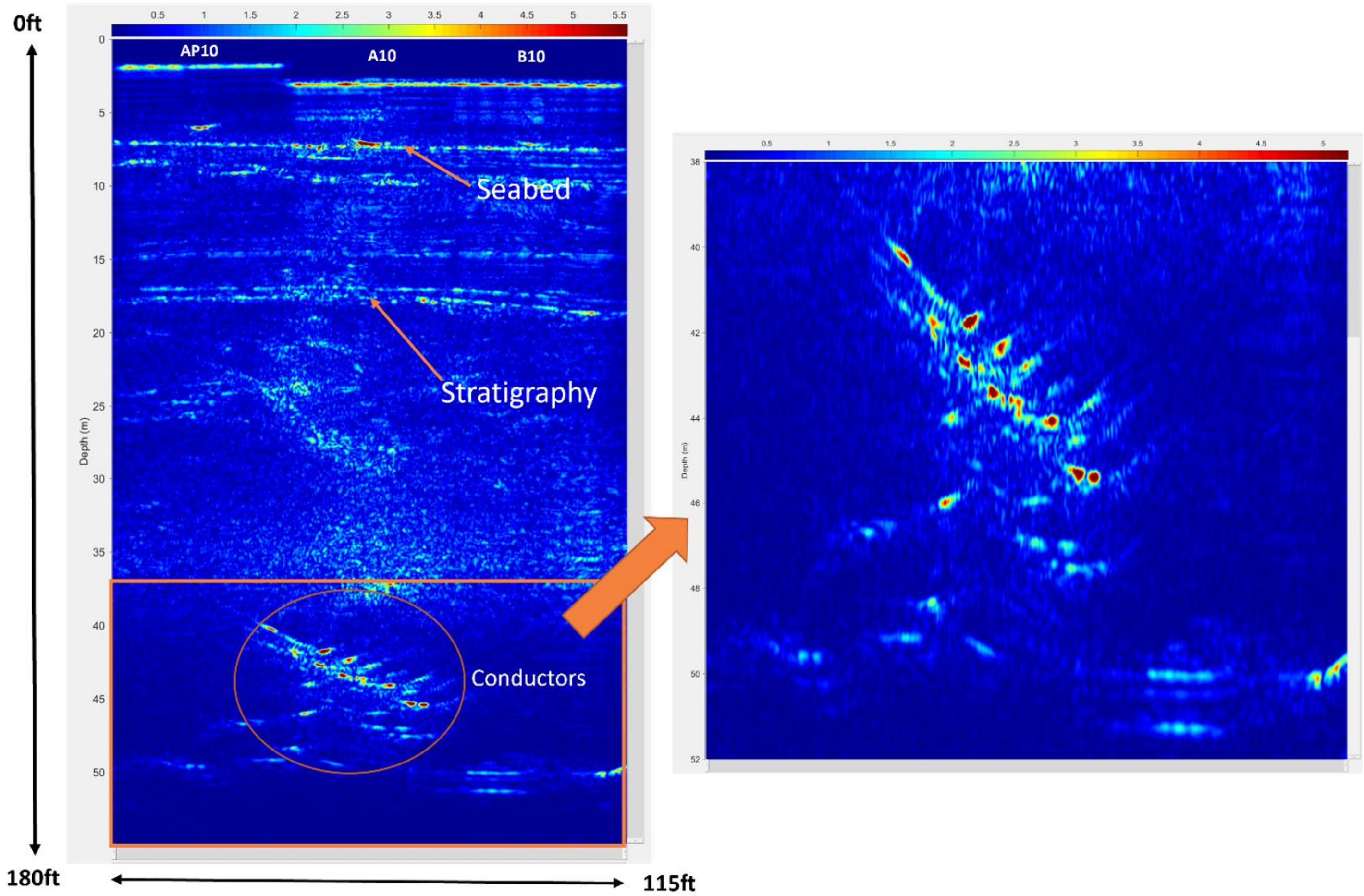

Figure 9 - Vertical section across Row 10 (Line B-B' in Figure 1). Strongly coherent sedimentary layering in the upper 20m is seen in the profile across Row 10 with a strong basement reflector

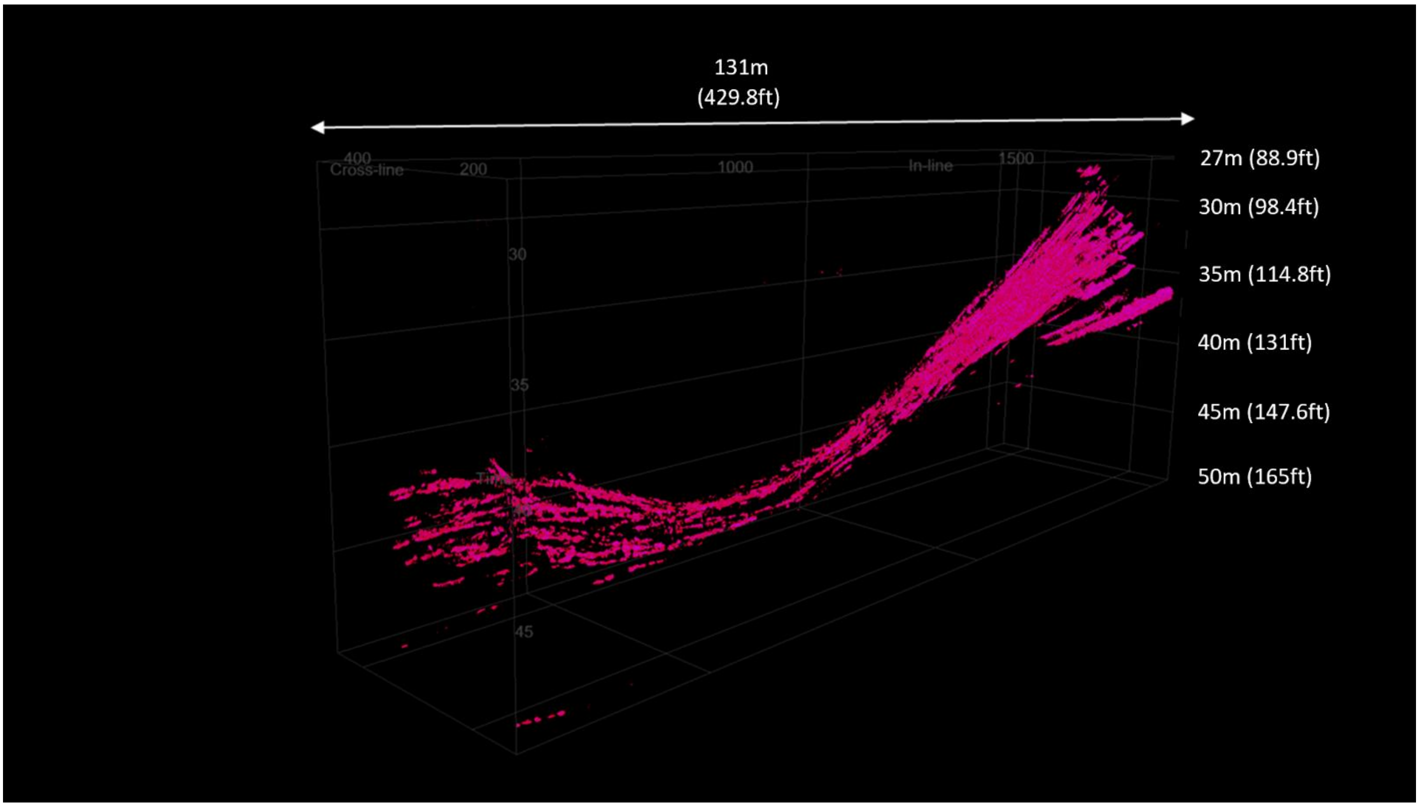

Figure 8 - Identified conductors as seen in the unified migrated volume

5 Conclusions

The approach of fusing in a cellular manner and not as mosaic data sets resulted in augmented clarity over a large volume of the sub-seabed. This enabled a higher level of detail in the distribution of geological and geotechnical properties including the nature of geohazards and stratigraphy. This is evident by the way the buried conductors were able to be captured and delineated for the first time. This methodology has the potential for windfarms foundation and risk mitigations.

6 Acknowledgements

The authors would like to thank the offshore geoscientists and operations team of Kraken Robotics for the collection and initial handling of this dataset.

7 References

Beylkin G. (1985). Imaging of Discontinuities in the Inverse Scattering Problem by Inversion of a Causal Generalized Radon Transform. J. Math. Phys. 26 (1).

Clark JI and Guigné JY. (1988). Marine Geotechnical Engineering in Canada. Canadian Geotechnical Journal. 25 (2), 179-198.

Guigné JY. (1986). The Concept, Design and Experimental Evaluation of Acoustic Sub-seabed Interrogation. Ph.D. thesis, University of Bath, Bath, UK.

Guigné JY and Chin VH. (1989). Acoustic Imaging of an Inhomogeneous Sediment Matrix. Marine Geophysical Researchers. 11, 301-317.

Guigné JY, Welford JK and McDermott IR. (2010). Volumetric, Multi-fold Acoustic Interrogations of Complex Sub-seabeds. Near Surface, EAGE – Zurich.

Guigné JY, Welford JK, Gogacz A and Clements C. (2012). US Patent Application- Method for Accentuating Specular and Non-Specular Seismic Events from within Shallow Subsurface Rock Formations.

Guigné JY. (2014). Acoustic Interrogations of Complex Seabeds. D.Sc. Thesis. University of Bath, Bath, UK.

Guigné JY and Blondel P. (2017). Acoustic Interrogations of Complex Seabeds. Springer Briefs, Heidelberg.

Inkpen ST, English J, Pike CJ, Guigné JY, Guzzwell J, Hunt P and Tuff K. (1991). A Three-dimensional Acoustic Site Surveying Probe. OTC 91, 23rd Annual Offshore Technology Conf Procs. Vol 1, Ppr OTC 6559, pp. 525-535.